Cholesterol Accumulation and Liver Cell Death in Mice With Niemann-Pick Type C Disease

Eduardo P. Beltroy,[1] James A. Richardson,[2] Jay D. Horton,[3,4] Stephen D. Turley,[3] and John M. Dietschy[3]

Niemann-Pick type C (NPC) disease develops as a result of mutations in the *NPC1* gene that encodes a protein involved in the net movement of unesterified cholesterol from the late endosomal/lysosomal compartment to the metabolically active pool of sterol in the cytosol of virtually every cell in the body. Although early publications emphasized the neurodegeneration occurring in children with this mutation, more recent clinical information suggests that serious liver disease also is an important part of this syndrome. These studies, therefore, were undertaken to characterize the liver dysfunction seen in mice with this same mutation. The NPC mouse develops significant hepatomegaly that reaches 8% of body weight at 5 to 6 weeks of age. This increase in liver size is associated with a linear increase in cholesterol content and with accumulation of amorphous cellular inclusions in both hepatocytes and macrophages. During the few weeks after birth, significant elevation of the plasma alkaline phosphatase level occurs, as also is seen in the human infant with this disease. At 4 to 5 weeks of age, plasma aminotransferase levels also rise abruptly. Histologically, at this time there is apoptosis, but no excess deposition of collagen or glycogen. mRNA expression is elevated for caspase 1, caspase 6, and several enzymes associated with sterol biosynthesis and bile acid formation. In conclusion, the NPC mouse has liver disease similar to that seen in the NPC infant and represents a relevant model for exploring the molecular events occurring in this form of liver disease. (HEPATOLOGY 2005;42:886-893.)

Niemann-Pick type C (NPC) disease is an autosomal recessive lipid storage disorder characterized by enlargement of the liver and spleen, progressive hepatic and neurological deterioration, and death in the second or third decade of life.[1] The mutation responsible for approximately 95% of these cases has been mapped to a gene on chromosome 18q11 designated *NPC1*.[2] This gene encodes a protein (NPC1) with 5 transmembrane domains that share homology with the sterol-sensing domain of 2 enzymes involved in cellular cholesterol homeostasis, 3-hydroxy-3-methylglutaryl coenzyme A reductase and sterol regulatory element binding protein cleavage-activating protein.[2,3]

Most cells in the body take up cholesterol from the surrounding environment, using one or more members of the low-density lipoprotein receptor (LDLR) family, and then process this sterol through the clathrin-coated pit pathway to the metabolically accessible pool of sterol in the cytosol.[4-6] Because the NPC1 protein apparently functions to move unesterified cholesterol from the late endosomal/lysosomal compartment of these cells to the metabolically active pool, the characteristic finding in the child (or mouse) with a mutation of this protein is the progressive accumulation of sterol in every tissue.[7-10] However, the magnitude of this accumulation varies in different organs, depending on how much cholesterol is normally taken up through the clathrin-coated pit pathway in each of these particular tissues.[11]

Liver plays the key role in the clearance of circulating cholesterol carried in lipoproteins and so manifests the highest rate of sterol accumulation in both the human and mouse with a mutation in *NPC1*.[5,7,9] The pathways responsible for this accumulation are outlined diagrammatically in Fig. 1. Cholesterol absorbed from the intestine and carried in the chylomicron remnant (CMr) is nearly completely cleared into the liver, using the LDLR and

Abbreviations: NPC, Niemann-Pick type C; NPC1, NPC1 protein; LDLR, low density lipoprotein receptor; CMr, chylomicron remnant; VLDLr, very low density lipoprotein remnant; LDL, low-density lipoprotein; HDL, high-density lipoprotein; SR-BI, scavenger receptor type BI, AP, alkaline phosphatase; AST, aspartate aminotransferase; ALT, alanine aminotransferase.

From the Departments of [1]Pediatrics, [2]Pathology, [3]Internal Medicine, and [4]Molecular Genetics, University of Texas Southwestern Medical School, Dallas, TX.

Received April 13, 2005; accepted July 17, 2005.

Supported by grants from the National Institutes of Health (R37 HL09610 and PO1 HL20948) and the Moss Heart Fund.

Address reprint requests to: John M. Dietschy, M.D., University of Texas Southwestern Medical Center, 5323 Harry Hines Blvd., Dallas, TX 75390-8887. E-mail: john.dietschy@utsouthwestern.edu; fax: 214-648-9761.

Published online in Wiley InterScience (www.interscience.wiley.com).

DOI 10.1002/hep.20868

Potential conflict of interest: Nothing to report.

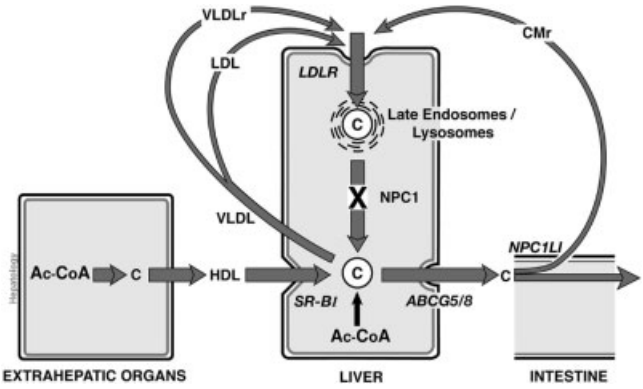

Fig. 1. Diagrammatical representation of the net flow of cholesterol through the various pathways and tissues of the NPC mouse. Cholesterol carried in LDL, VLDLr, and CMr is taken up into the liver cell by the LDLR and processed through the clathrin-coated pit. In the presence of a mutation in NPC1, the unesterified cholesterol from these particles becomes trapped in the late endosomal/lysosomal compartment and cannot be further metabolized or excreted. In contrast, cholesterol from HDL or sterol that is newly synthesized in the liver is processed normally through the metabolically active pool in the cytosol. ABCG5/8 and NPC1L1 represent the cholesterol transporter in the biliary canaliculus and intestine, respectively. NPC, Niemann-Pick type C; LDL, low-density lipoprotein; VLDLr, very low density lipoprotein remnant; CMr, chlyomicron remnant; LDLR, low-density lipoprotein receptor; HDL, high-density lipoprotein.

clathrin-coated pit pathway. Similarly, nearly all of the cholesterol carried in the remnant of very low density lipoprotein (VLDLr) and approximately 80% of the sterol in low-density lipoprotein (LDL) is cleared from the plasma by the liver.[5,12] Nearly all of this sterol becomes trapped in the late endosomal/lysosomal compartment when NPC1 is mutated and not functional. In contrast, as also shown in Fig. 1, cholesterol that is carried in high-density lipoprotein (HDL) and taken up into the liver by scavenger receptor BI (SR-BI) or that is synthesized in the hepatocyte is handled normally by the liver.[13]

Despite significant advances in understanding the pathogenesis of NPC disease, the liver dysfunction associated with this syndrome has been largely ignored and is poorly characterized. However, the literature suggests that between 45% and 65% of NPC patients present with neonatal cholestasis, and 10% of these will die of liver failure before 6 months of age.[14-16] These patients typically do not have neurological manifestations. In another study, NPC disease was found to be the second most common genetic/metabolic cause of neonatal cholestasis after alpha-1-antitrypsin deficiency over a 20-year period at King's College Hospital in the United Kingdom.[17] In a retrospective review over a 2-year period in the United States, NPC disease was the most common genetic/metabolic cause of neonatal cholestasis.[15] Such data suggest that severe liver dysfunction in NPC disease is more common than previously believed.

Because of the potential significance of this liver disorder in children with the *NPC1* mutation, the current studies were undertaken to define the liver dysfunction present in a murine model of NPC disease, the BALB/c mouse with a mutation in the *npc1* gene. This model has proved valuable in delineating many of the molecular and physiological defects found in the presence of the *npc1* mutation and in testing potential therapies to reverse these defects. However, only one report has appeared of the hepatic lesions seen in this murine model, and this study was carried out in animals fed a very high-fat, high-cholesterol diet.[18] For this reason, the current studies were undertaken to delineate in detail the biochemical, histological, and molecular abnormalities that occur in the liver of the NPC mouse maintained on low levels of dietary lipid intake.

Materials and Methods

Animals and Diets. Wild type ($npc1^{+/+}$) and homozygous mutant ($npc1^{-/-}$) mice were generated from heterozygous $npc1^{+/-}$ animals with a BALB/c background. Breeding stock was originally obtained from Dr. Peter G. Pentchev at the National Institutes of Health.[3] All animals were fed *ad libitum* a low-cholesterol rodent diet (no. 7001; Harlan Teklad, Madison, WI) after weaning at 19 days of age. This diet had a cholesterol content of 0.016% (wt/wt) and a total lipid content of 5% (wt/wt). Measurements were made in animals at different ages, varying from 1 to 75 days. Because no gender differences were observed in any experimental parameter, the experimental groups consisted of equal or nearly equal numbers of males and females. All experimental protocols were approved by the Institutional Animal Care and Use Committee.

Measurement of Tissue Cholesterol Concentration. Animals were exsanguinated, and the brain and liver were removed and saponified. The sterol was extracted with petroleum ether, and the cholesterol concentration was measured by gas-liquid chromatography using stigmastanol (Sigma, St. Louis, MO) as an internal standard.[19,20] The values were expressed either as milligrams of cholesterol per gram wet weight of tissue (mg/g) or as milligrams of cholesterol per whole organ (mg/whole organ).

Measurement of Liver Triacylglycerol Content. An aliquot of liver (300-400 mg) was extracted in chloroform:methanol (2:1, vol/vol) in the presence of [^{14}C]triolein (American Radiolabeled Chemicals, Inc., St. Louis, MO). Duplicate 5-mL aliquots of this extract were dried under air, and the residue was redissolved in 1 mL hexane: methyl-t-butyl ether (100:1.5, vol/vol). This solution was run over a Sep-Pak Vac RC silica cartridge (500 mg) (Waters Corp., Milford, MA). After elution of the cho-

lesteryl esters, the solvent was changed to hexane:methyl-t-butyl ether (96:4, vol/vol) for elution of the triacylglycerols. This fraction was dried under air and redissolved in chloroform–methanol (2:1, vol/vol). Aliquots of this solution were dried and used for the measurement of the recovery of the internal standard, and the mass of triacylglycerol was measured using Infinity Triglycerides Liquid Stable reagent (ThermoTrace, Noble Park, Australia). This value was used to calculate the milligrams triacylglycerol in the whole liver.

Measurement of Plasma Liver Enzyme Activities. Plasma alkaline phosphatase, aspartate aminotransferase (AST), and alanine aminotransferase (ALT) activities (U/L) were measured by a commercial laboratory.

Histology. Livers were harvested from age-matched *npc1*$^{+/+}$ and *npc1*$^{-/-}$ mice at 5, 12, 56, and 75 days of age. Tissues were fixed in either 4% paraformaldehyde or alcoholic formalin,[21] and sections were then stained with hematoxylin-eosin, Masson Trichrome stain,[22] periodic acid-Schiff (PAS),[22] or for nuclear DNA fragmentation (terminal deoxynucleotidyl transferase-mediated nick-end labeling [TUNEL])[23].

Measurement of Relative mRNA Expression in Liver Tissue. Aliquots of liver tissue from animals at 56 days of age were frozen in liquid nitrogen. Total RNA was prepared from 4 liver samples of *npc1*$^{+/+}$ and *npc1*$^{-/-}$ mice, and equal aliquots were pooled with an RNA STAT-60 kit (Tel-Test, Friendswood, TX). cDNA was synthesized from 5 μg DNase I-treated total RNA (Rnase free, FPLC pure, Amersham Pharmacia, Buckinghamshire, UK) using the SuperScript First-Strand Synthesis System (catalogue no. 11904-018, GIBCO/BRL) and random hexamer primers. Specific primers for each gene were designed by using PRIMER EXPRESS software (Perkin-Elmer, Boston, MA). The real-time reverse transcription polymerase chain reaction contained, in a final volume of 30 μL, 50 ng reverse-transcribed total RNA, 167 nmol forward and reverse primers, and 15 μL 2$\times$ SYBR green PCR Master Mix.[24] PCRs were carried out by using the Applied Biosystems Prism 7700 Sequence Detection System (Foster City, CA). All reactions were done in triplicate. The relative amounts of all mRNAs were calculated using the comparative C_T method (User Bulletin no. 2, Perkin-Elmer).

Measurement of Cholesterol and Fatty Acid Synthesis. The rates of cholesterol and fatty acid synthesis were measured *in vivo* by using [^{3}H]water as previously described.[20]

Results

Whole Body and Organ Size During Development. Initial experiments were undertaken to quantify the effect of the *npc1* mutation on the growth of the whole animal, and on the absolute and relative weights of the liver and brain, the two organs primarily affected by this disease. As shown in Fig. 2A, the *npc1*$^{+/+}$ and *npc1*$^{-/-}$ animals progressively gained weight over most of the 75 days of observation, although a pause occurred in the rate of gain in both groups just as the animals were weaned to solid food. However, the mean weights of the *npc1*$^{-/-}$ animals were lower than those of the *npc1*$^{+/+}$ mice at nearly every age, and these differences became large between 49 and 75 days of age, when significant neurological abnormalities became manifest. In contrast, throughout this period of growth, the mean weight of the liver in the *npc1*$^{-/-}$ mice equaled or exceeded that seen in the control mice (Fig. 2B). These differences were even greater when relative liver weight was calculated (Fig. 2C). Relative liver size declined during the first 2 weeks of life as the mice went into a period of rapid body growth. Beyond this age, however, relative liver size increased, and this increase was greater in the *npc1*$^{-/-}$ animals than in the control mice. After approximately 42 days of age, the liver accounted for approximately 6% of body weight in the *npc1*$^{+/+}$mice but 8% in the *npc1*$^{-/-}$ animals. The absolute weight of the brain was less in mutant mice (Fig. 2D). However, when corrected for the lower body weights seen in these *npc1*$^{-/-}$ animals, relative brain weight was the same in the mutant and control mice (Fig. 2E).

Liver and Brain Cholesterol Concentration and Content. The striking effect of the *npc1* mutation on sterol homeostasis is evident in Fig. 3. In the *npc1*$^{+/+}$mice, the concentration of cholesterol was elevated at approximately 4 mg/g during the suckling period but promptly fell to approximately 2.2 mg/g after weaning when oral cholesterol intake decreased (A). In contrast, in the *npc1*$^{-/-}$ mice, this concentration was much higher at every age, although these values temporarily declined after weaning before again increasing in the older animals. This variation in concentration resulted from the variable rate of liver growth during this same period (Fig. 2B). A more accurate assessment of the absolute rate of cholesterol accumulation in the liver of the animals with the *npc1* mutation is seen when whole organ sterol content is calculated. As is apparent, the absolute amount of cholesterol in the liver increased in an essentially linear manner from 0.8 mg at birth to 37 mg at 56 days of age (Fig. 3B). However, the content of cholesterol in the liver of the *npc1*$^{+/+}$ animals increased from only 0.4 mg to 3.6 mg over this same interval. In contrast to these findings in the liver, the concentration of cholesterol in the brain of the *npc1*$^{-/-}$ animals was marginally less than in the control mice at all ages beyond approximately 28 days (Fig. 3C), and this difference was even greater when whole brain sterol content was calculated (Fig. 3D). This decrease represented the nerve cell death and demyeli-

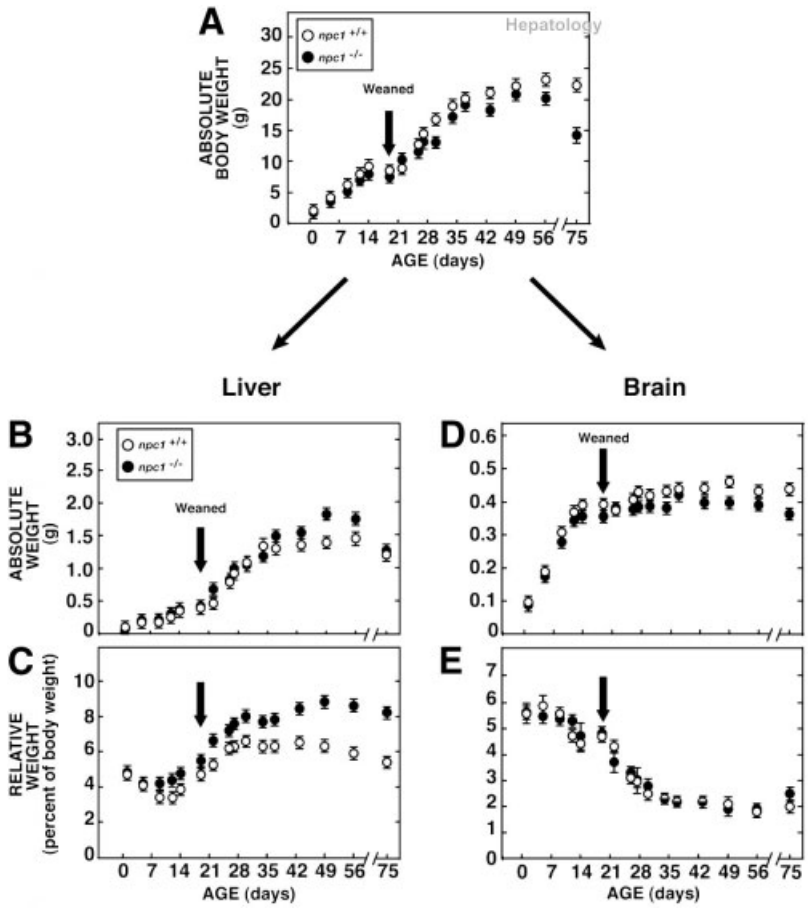

Fig. 2. Whole body, liver, and brain weights in *npc1*$^{+/+}$ and *npc1*$^{-/-}$ mice at different ages. Absolute body (A), liver (B), and brain (D) weights of animals from 1 to 75 days of age are shown. The weights of the liver (C) and brain (E) are also presented as a percentage of whole body weight. As shown by the arrows, the mice were weaned at 19 days of age to the rodent diet. Each data point represents the mean ± SEM of values for 6 to 12 animals in each group. The experimental groups contained nearly equal numbers of males and females.

nation known to be occurring at these ages in the *npc1*$^{-/-}$ animals.[25-27]

Assessment of Liver Cell Damage. The plasma level of 3 enzymes was next measured to assess liver cell damage in these same groups of animals. As seen in Fig. 4A, the plasma alkaline phosphatase (AP) level was elevated in both groups of newborn pups, although the value was higher in the *npc1*$^{-/-}$ mice (815 U/L) than in the control animals (578 U/L). However, this value progressively declined in the *npc1*$^{+/+}$ mice over the next 28 days, but

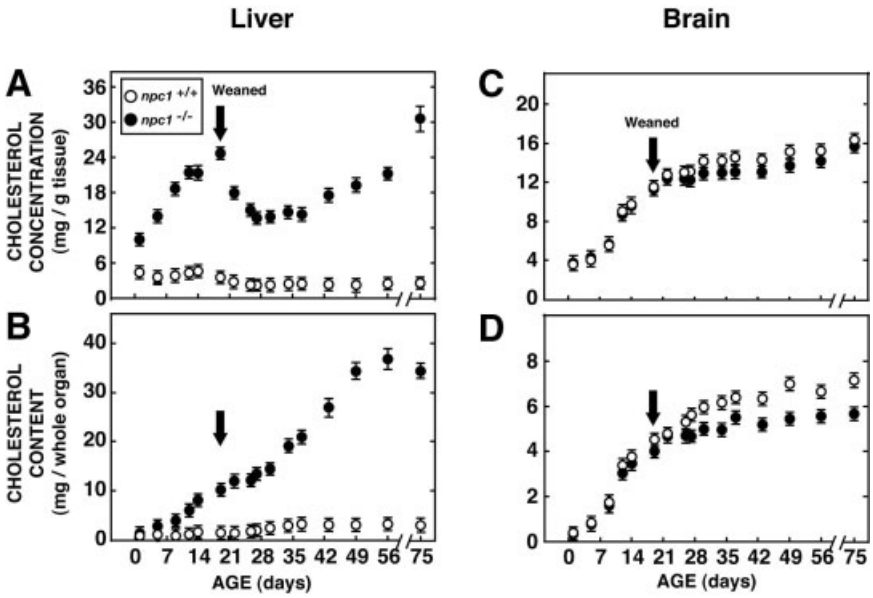

Fig. 3. Liver and brain cholesterol concentration and content in *npc1*$^{+/+}$ and *npc1*$^{-/-}$ mice of different ages. Mice from 1 to 75 days of age were killed, and the amount of cholesterol present in the liver and brain was measured. These data are expressed as both cholesterol concentration (A,C) and total sterol content (B,D). Each data point represents the mean ± SEM for 6 to 12 animals in each group.

increased abruptly (to 965 U/L) in the mutant animals before returning to much lower levels in the older mice. In contrast, the plasma levels of both ALT and AST were normal or only minimally elevated during this initial 28-day period. However, both enzymes began to increase dramatically at approximately 35 days of age, reaching values in the mutant mice that were approximately 15-fold higher than those seen in the control animals at 75 days of age (Fig. 4B-C).

Hepatic Histology. To correlate these changes in hepatic cholesterol accumulation and plasma enzyme levels with cellular damage, histological examination of the liver was next carried out at several critical times during the evolution of this disease. As seen in Fig. 5A-B, at 5 days of age there was no observable difference in liver histology in the *npc1*$^{-/-}$ mice even though the cholesterol content of these cells was already significantly elevated (2.7 vs. 0.7 mg/whole organ) compared with the control mice. Foci of extramedullary hematopoiesis were seen. No evidence was seen of inflammation or cholestasis in either group of animals. At 12 days of age, when the cellular cholesterol content was further elevated (6.0 vs. 1.2 mg/whole organ) the hepatocytes were swollen and showed finely vacuolated cytoplasm (Fig. 5C-D). Within the sinusoids, small numbers of large, pale-stained macrophages were identified. In addition, increased numbers of hepatocytes in mitosis were seen in the sections from the *npc1*$^{-/-}$ mice, but not in those from the *npc1*$^{+/+}$ animals. No evidence was seen of periportal inflammation. At 56 days of age (36.8 vs. 3.3 mg/whole organ), differences were more dramatic (Fig. 5E-F). Large numbers of foamy macrophages were seen within the sinusoids of the livers from the *npc1*$^{-/-}$ animals, and, commonly, these macrophages were in clusters of 3 to 4 cells. Apoptosis of hepatocytes was common, but mitotic activity was rare. Again, there was no evidence of periportal inflammation. At 75 days of

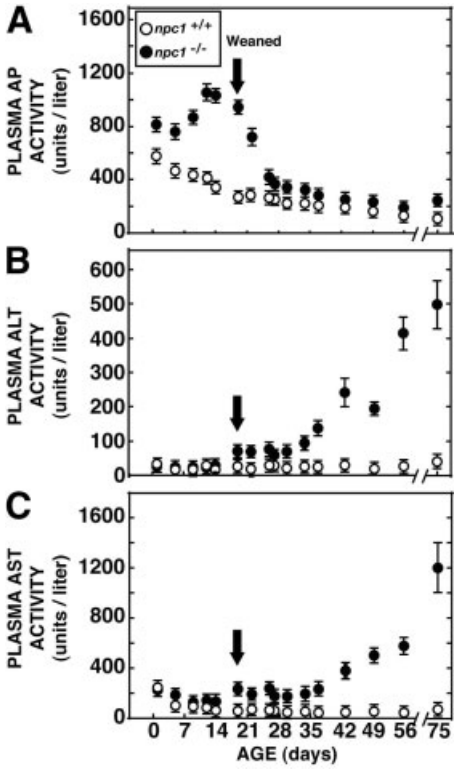

Fig. 4. Plasma liver enzyme activities in *npc1*$^{+/+}$ and *npc1*$^{-/-}$ mice at different ages. The plasma levels of alkaline phosphatase (A), alanine aminotransferase (B), and aspartate aminotransferase (C) activities were measured in the same groups of mice that were used to obtain the data in Fig. 3. Each data point represents the mean ± SEM for 6 to 12 animals in each group.

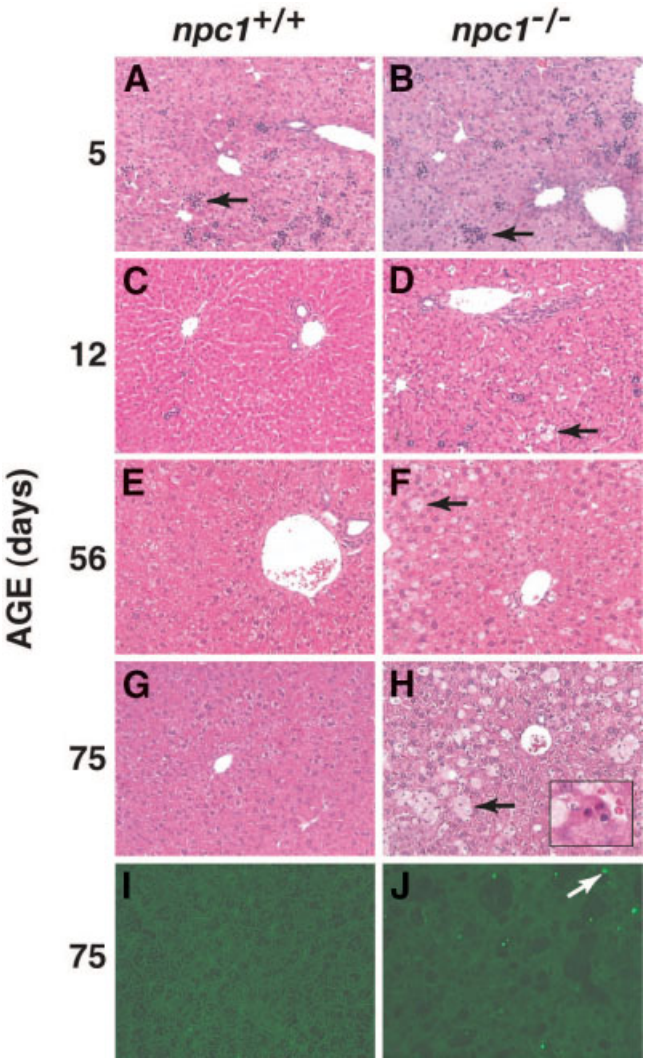

Fig. 5. Liver histopathology in *npc1*$^{+/+}$ and *npc1*$^{-/-}$ mice at different ages. Hematoxylin-eosin–stained liver sections from *npc1*$^{+/+}$ and *npc1*$^{-/-}$ animals at 5, 12, 56, and 75 days of age are shown (20× magnification) (A-H). An apoptotic body is seen in the insert (H) (magnification ×40). TUNEL stains of liver sections from 75-day-old animals are also presented (I-J). The arrows point to clusters of hematopoietic cells (A-B), lipid-laden macrophages (D,F,H), or nuclei undergoing programmed cell death (J).

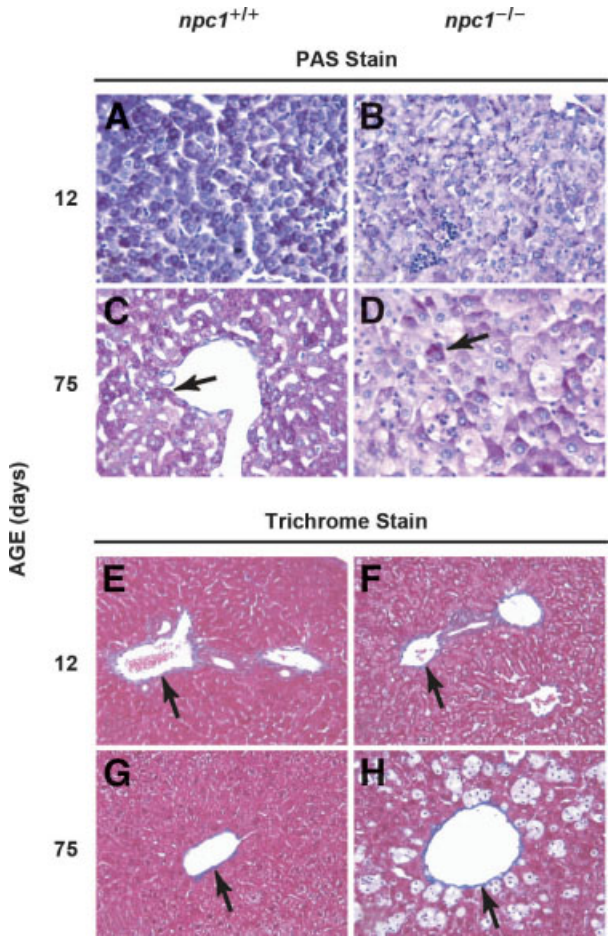

Fig. 6. Glycogen and collagen staining in liver sections of *npc1*$^{+/+}$ and *npc1*$^{-/-}$ mice at different ages. Liver sections of *npc1*$^{+/+}$ and *npc1*$^{-/-}$ animals at 12 and 75 days of age were stained with PAS and Masson Trichrome stain to detect the presence of glycogen (dark purple) and collagen (blue), respectively. The arrows point to periodic acid-Schiff–positive inclusions (C-D) and collagen deposition (E-H).

age (34.4 vs. 2.9 mg/whole organ), the number of sinusoidal macrophages increased further to represent approximately one third of the cross-sectional area of the sections examined. Apoptosis was common in macrophages and hepatocytes (Fig. 5G-H), and fragmented nuclear DNA was identified on TUNEL-stained sections (Fig. 5I-J).

PAS staining showed minimal accumulation of glycogen in the hepatocytes of the *npc1*$^{-/-}$ animals at 12 days of age (Fig. 6A-B). Furthermore, the amount of glycogen accumulation seen in these 12-day-old animals was not different from that observed in the *npc1*$^{-/-}$ mice at 75 days of age (Fig. 6B,D). Liver samples obtained from 12-day-old animals and stained with trichrome stain showed only minimal collagen deposition, mainly around the central veins, and there were no apparent differences in the livers from the mutant and control mice (Fig. 6E-F). Furthermore, no significant increase was seen in collagen deposition even in the *npc1*$^{-/-}$ animals at 75 days of age (Fig. 6G-H), as has been previously reported.[28]

Hepatic Lipid Content and Synthesis, and Expression of mRNA Levels. Finally, several metabolic parameters and the relative mRNA expression for a number of proteins were measured in 56-day-old *npc1*$^{+/+}$ and *npc1*$^{-/-}$ mice, as shown in Fig. 7. The content of cholesterol (panel A) was very high, as was the rate of sterol synthesis (panel B) in the *npc1*$^{-/-}$ animals. However, the content of triacylglycerol (panel C) and the rate of fatty acid synthesis (panel D) were lower in the mutant than in the control mice. This difference in the rate of cholesterol synthesis was reflected in the relative mRNA expression in the *npc1*$^{-/-}$ animals for HMGCoA reductase (HMG-CoAR) (panel E), the rate-limiting enzyme in the biosynthetic pathway. Importantly, the relative mRNA levels for tumor necrosis factor alpha (panel F), caspase 1 (panel G), and caspase 6 (panel H) were also elevated in the livers of the mutant mice.

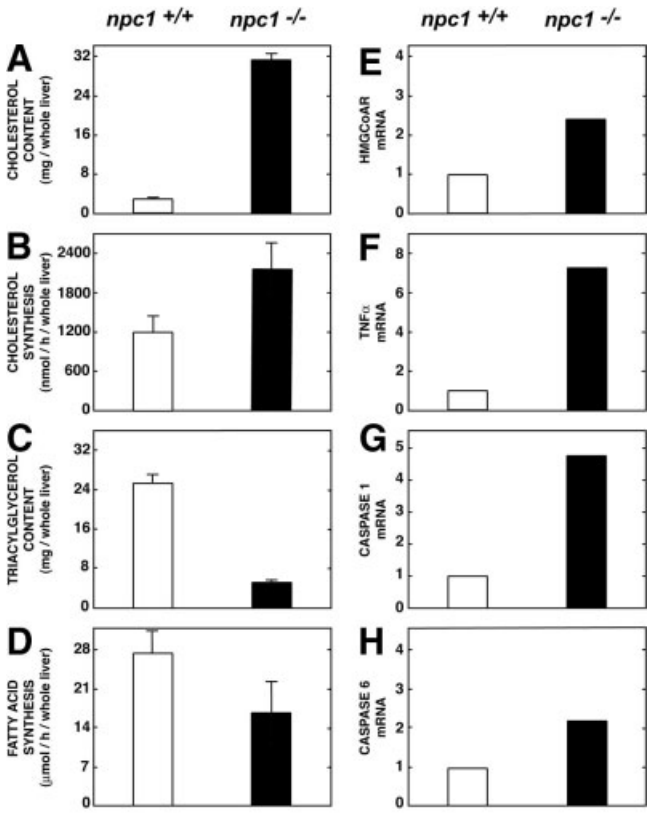

Fig. 7. Cholesterol and fatty acid synthesis and content, and mRNA relative expression for various proteins in the liver of 56-day-old *npc1*$^{+/+}$ and *npc1*$^{-/-}$ animals. The content of both cholesterol (A) and triacylglycerol (C) and the rate of sterol (B) and fatty acid (D) synthesis are shown. The level of expression of mRNA for a variety of proteins is also illustrated (E-H). In these latter measurements, the mRNA relative expression level in the *npc1*$^{+/+}$ animals was always set at 1.0. The data in panels A through D represent means ± SEM for 6 to 10 animals in each group. The data in panels E through H are the values obtained from pooled samples from 4 animals in each group.

Discussion

The physiological characteristics of the phenotype of the *npc1*$^{-/-}$ animal (and human) are very unusual, as illustrated by these studies. The fundamental problem caused by mutation of the NPC1 protein is that unesterified cholesterol, derived from apoB-containing lipoproteins processed through the clathrin-coated pit pathway, becomes trapped in late endosomes/lysosomes (Fig. 1). In contrast, cholesterol newly synthesized in the extrahepatic organs and delivered to the liver through the SR-BI pathway is processed normally to biliary sterols and bile acids (Fig. 1).[13] Because the sterol trapped in the late endosomal/lysosomal compartment cannot become part of the metabolically active pool in the cell, paradoxically, the hepatocyte senses a shortage of cholesterol and, to compensate, increases the rate of synthesis. Thus, in the face of a massively expanded hepatic cholesterol pool (Figs. 3B, 7A), an increase occurs in the relative mRNA expression of HMGCoAR (Fig. 7E), the rate-limiting enzyme in the biosynthetic pathway, and a corresponding increase in overall sterol synthesis (Fig. 7B). In this manner, sterol balance across the liver and whole animal is maintained, but the mass of unesterified cholesterol in the late endosomal/lysosomal compartment progressively expands with age (Fig. 3B).

This expansion clearly leads to significant abnormalities of liver function. During the suckling period, when both absolute (Fig. 2B) and relative (Fig. 2C) hepatic growth is slow and the intake of dietary sterol from milk is high, the concentration of cholesterol in the liver of the pups increases abruptly (Fig. 3A). This increase is associated with a similar marked rise in the plasma alkaline phosphatase level that then returns toward normal in the older animals (Fig. 4A). Notably, most (65% in one series[14]) newborn infants with NPC disease also manifest prolonged cholestasis that usually disappears with age.[14,15,29] Only later in the young adult mice do the aminotransferase levels increase significantly (Fig. 4B-C) at a time when there is also an increase in the relative mRNA expression of tumor necrosis factor alpha and caspases 1 and 6 (Fig. 7F-H) and the histological appearance of apoptotic cells (Fig. 5H,J). This finding again is similar to reports in humans with NPC disease that approximately half of those children who recover from the period of prolonged neonatal cholestasis manifest persistent liver disease with elevated aminotransferase levels.[14]

Similarities also were seen in the histology of the diseased liver in the mice and humans. Both species show vesicular cytosolic inclusions, activation of sinusoidal macrophages, and apoptotic cells (Fig. 5).[14,15] In some young children, however, increased fibrotic tissue has been described in liver biopsies with interlobular and intralobular bridging and, in some cases, full-blown cirrhosis.[14,15] In contrast, there was no increase in hepatic fibrosis in the *npc1*$^{-/-}$ mice detected by trichrome staining (Fig. 6H). However, a two-fold increase in hepatic hydroxyproline content has been reported in such animals even though excess fibrosis could not be detected histologically.[28] Because these animals developed obvious neurological symptoms beginning at 5 to 6 weeks and died at 11 to 12 weeks of age, possibly there was insufficient time for the development of detectable fibrosis even though there was significant liver cell damage in this murine model.

These findings in the liver differ in several respects from those in the brain. As in the liver, there is accumulation of unesterified cholesterol in the neurons of the central nervous system with selective cell death.[10,25,27,30] Unlike the liver, however, this neurodegeneration is associated with demyelination so that the mass of unesterified cholesterol in the central nervous system decreases slightly (Fig. 3D) rather than increasing, as it does in the liver (Fig. 3B).[30] However, as these studies show, the mice and humans with NPC disease both develop hepatic and neurological dysfunction. However, which factors determine the relative severity of each of these lesions in a given individual is not clear. Children who initially manifest significant liver abnormalities apparently die at a median age of 8.3 years, whereas those who have predominantly neurological symptoms die at a median age of 10.5 years.[14]

In conclusion, these and other studies indicate that this murine model represents a very useful experimental animal in which to further explore the pathogenesis of both the liver and central nervous system disease. Furthermore, because the mechanisms of cholesterol delivery to the liver are now well understood and because new pharmaceutical agents are available to interrupt this delivery, it may be possible in the near future to design therapy that will considerably ameliorate the severity of the liver disease and so improve the quality of life for children with NPC disease.

Acknowledgment: The authors thank Claire Havel, Jennifer Weissblum and Norma Anderson for excellent technical assistance and Merikay Presley for expert preparation of the manuscript.

References

1. Brady RO, Carstea ED, Pentchev PG: The Niemann-Pick Diseases Group. In: Rosenberg RN, Prusiner SB, DiMauro S, Barchi RL, eds. The Molecular and Genetic Basis of Neurological Disease. 2nd ed. Boston: Butterworth-Heinmann, 1997:387-403.

2. Carstea ED, Morris JA, Coleman KG, Loftus SK, Zhang D, Cummings C, et al. Niemann-Pick C1 disease gene: homology to mediators of cholesterol homeostasis. Science 1997;277:228-231.
3. Loftus SK, Morris JA, Carstea ED, Gu JZ, Cummings C, Brown A, et al. Murine model of Niemann-Pick C disease: mutation in a cholesterol homeostasis gene. Science 1997;277:232-235.
4. Goldstein JL, Dana SE, Faust JR, Beaudet AL, Brown MS. Role of lysosomal acid lipase in the metabolism of plasma low density lipoprotein. J Biol Chem 1975;250:8487-8495.
5. Osono Y, Woollett LA, Herz J, Dietschy JM. Role of the low density lipoprotein receptor in the flux of cholesterol through the plasma and across the tissues of the mouse. J Clin Invest 1995;95:1124-1132.
6. Herz J, Bock HH. Lipoprotein receptors in the nervous system. Annu Rev Biochem 2002;71:405-434.
7. Pentchev PG, Vanier MT, Suzuki K, Patterson MC. Niemann-Pick disease type C: a cellular cholesterol lipidosis. In: Scriver CR, Beaudet AL, Sly WS, Valle D, Stanbury JB, Wyngaarden JB, et al., eds. The Metabolic and Molecular Bases of Inherited Diseases. Vol. 2. 7th ed. New York: McGraw-Hill, 1995:2625-2639.
8. Neufeld EB, Wastney M, Patel S, Suresh S, Cooney AM, Dwyer NK, et al. The Niemann-Pick C1 protein resides in a vesicular compartment linked to retrograde transport of multiple lysosomal cargo. J Biol Chem 1999; 274:9627-9635.
9. Xie C, Turley SD, Pentchev PG, Dietschy JM. Cholesterol balance and metabolism in mice with loss of function of Niemann-Pick C protein. Am J Physiol 1999;276:E336-E344.
10. Reid PC, Sakashita N, Sugii S, Ohno-Iwashita Y, Shimada Y, Hickey WF, et al. A novel cholesterol stain reveals early neuronal cholesterol accumulation in the Niemann-Pick type C1 mouse brain. J Lipid Res 2004;45: 582-591.
11. Xie C, Turley SD, Dietschy JM. Cholesterol accumulation in tissues of the Niemann-Pick type C mouse is determined by the rate of lipoprotein-cholesterol uptake through the coated-pit pathway in each organ. Proc Natl Acad Sci U S A 1999;96:11992-11997.
12. Spady DK, Huettinger M, Bilheimer DW, Dietschy JM. Role of receptor-independent low density lipoprotein transport in the maintenance of tissue cholesterol balance in the normal and WHHL rabbit. J Lipid Res 1987; 28:32-41.
13. Xie C, Turley SD, Dietschy JM. Centripetal cholesterol flow from the extrahepatic organs through the liver is normal in mice with mutated Niemann-Pick type C protein (NPC1). J Lipid Res 2000;41:1278-1289.
14. Kelly DA, Portmann B, Mowat AP, Sherlock S, Lake BD. Niemann-Pick disease type C: Diagnosis and outcome in children, with particular reference to liver disease. J Pediatr 1993;123:242-247.
15. Yerushalmi B, Sokol RJ, Narkewicz MR, Smith D, Ashmead JW, Wenger DA. Niemann-Pick disease type C in neonatal cholestasis at a North American center. J Pediatr Gastroenterol Nutr 2002;35:44-50.
16. Vanier MT, Millat G. Niemann-Pick disease type C. Clin Genet 2003;64: 269-281.
17. Mieli-Vergani G, Howard ER, Mowat AP. Liver disease in infancy: a 20 year perspective. Gut 1991;Suppl:S123-S128.
18. Erickson RP, Bhattacharyya A, Hunter RJ, Heidenreich RA, Cherrington NJ. Liver disease with altered bile acid transport in Niemann-Pick C mice on a high fat, 1% cholesterol diet. Am J Physiol 2005;289:G300-G307.
19. Turley SD, Herndon MW, Dietschy JM. Reevaluation and application of the dual-isotope plasma ratio method for the measurement of intestinal cholesterol absorption in the hamster. J Lipid Res 1994;35:328-339.
20. Schwarz M, Russell DW, Dietschy JM, Turley SD. Marked reduction in bile acid synthesis in cholesterol 7α-hydroxylase-deficient mice does not lead to diminished tissue cholesterol turnover or to hypercholesterolemia. J Lipid Res 1998;39:1833-1843.
21. Shehan DC, Hrapchak BB. Theory and Practice of Histotechnology. 2nd ed. Columbus, Ohio: Battelle Press, 1980:59-85.
22. Carson FL. Histotechnology. A Self-Instructional Text. Chicago: American Society for Clinical Pathology Press, 1997.
23. Gavrieli Y, Sherman Y, Ben-Sasson SA. Identification of programmed cell death in situ via specific labeling of nuclear DNA fragmentation. J Cell Biol 1992;119:493-501.
24. Liang G, Yang J, Horton JD, Hammer RE, Goldstein JL, Brown MS. Diminished hepatic response to fasting/refeeding and liver X receptor agonists in mice with selective deficiency of sterol regulatory element-binding protein-1c. J Biol Chem 2002;277:9520-9528.
25. Xie C, Burns DK, Turley SD, Dietschy JM. Cholesterol is sequestered in the brains of mice with Niemann-Pick Type C disease but turnover is increased. J Neuropathol Exp Neurol 2000;59:1106-1117.
26. Xie C, Lund EG, Turley SD, Russell DW, Dietschy JM. Quantitation of two pathways for cholesterol excretion from the brain in normal mice and mice with neurodegeneration. J Lipid Res 2003;44:1780-1789.
27. Li H, Repa JJ, Valasek MA, Beltroy EP, Turley SD, German DC, et al. Molecular, anatomical and biochemical events associated with neurodegeneration in mice with Niemann-Pick type C disease. J Neuropathol Exp Neurol 2005;64:323-333.
28. Guo J, Erickson R, Trouard T, Galons JP, Gillies R. Magnetization transfer contrast imaging in Niemann Pick type C mouse liver. J Magn Reson Imaging 2003;18:321-327.
29. Vanier MT, Suzuki K. Recent advances in elucidating Niemann-Pick C disease. Brain Pathol 1998;8:163-174.
30. Dietschy JM, Turley SD. Cholesterol metabolism in the central nervous system during early development and in the mature animal. J Lipid Res 2004;45:1375-1397.